
Transmuting prompts into weights

Hanna Mazzawi*
 Google Research
 mazzawi@google.com

Benoit Dherin*
 Google Research
 dherin@google.com

Michael Munn*
 Google Research
 munn@google.com

Michael Wunder
 Google Research
 mwunder@google.com

Javier Gonzalvo
 Google Research
 xavigonzalvo@google.com

Abstract

A growing body of research has demonstrated that the behavior of large language models can be effectively controlled at inference time by directly modifying their internal states, either through vector additions to their activations or through updates to their weight matrices. These techniques, while powerful, are often guided by empirical heuristics, such as deriving “steering vectors” from the average activations of contrastive prompts. This work provides a theoretical foundation for these interventions, explaining how they emerge from the fundamental computations of the transformer architecture. Building on the recent finding that a prompt’s influence can be mathematically mapped to *token-dependent* implicit weight updates (Dherin et. al, 2025), we derive a principled method for condensing this information into *token-independent* thought vectors and thought matrices. These constructs provide a theoretical explanation for existing vector-and-matrix-based model editing techniques and offer a direct, computationally-grounded method for transmuting textual input into reusable weight updates.

1 Introduction

Recent advancements in controlling large language models have moved beyond prompt engineering to a paradigm of direct intervention in the model’s computational process at inference time. These methods can be broadly categorized into two families. The first, often called *activation steering*, involves adding carefully crafted “steering vectors” to the hidden states of a model to guide its output towards a desired behavior, such as a particular sentiment or style (Subramani et al., 2022; Li et al., 2023). These vectors are typically computed using heuristic methods, for instance, by averaging the difference in activations between positive and negative example prompts (Turner et al., 2025; Todd et al., 2024). The second family of methods, known as *model editing*, seeks to instill new knowledge or behaviors by applying targeted, often low-rank, modifications directly to the model’s weight matrices, particularly those in the feed-forward layers (Meng et al., 2022; Mitchell et al., 2022).

While these intervention strategies have proven remarkably effective, their development has been largely empirical. The recipes for constructing steering vectors and weight matrices are powerful but lack a clear theoretical justification rooted in the transformer architecture itself. This raises a fundamental question: Why do interventions like averaging contrastive activations or applying low-rank matrix updates succeed in controlling complex model behaviors? What is the underlying mathematical principle that connects a textual instruction to a specific change in a model’s weights or activations?

*These authors contributed equally to this work

This work provides a theoretical framework that answers these questions by showing how a transformer natively processes prompt information by creating implicit, layer-by-layer updates to its own weights. Our analysis builds on the foundational result of Dherin et al. (2025), which proved that for a single transformer block, the computational effect of an input prompt can be perfectly replicated by applying specific, token-dependent updates to the block’s feed-forward weights. These updates naturally decompose into a vector component (a bias update) and a matrix component. Our primary contribution is to demonstrate how these transient, token-dependent patches can be aggregated into reusable weight updates that are independent of any specific input token. We call these distilled updates *thought vectors* (similar to steering vectors) denoted $\delta(\mathcal{I})$, and *thought matrices* (similar to matrix edits) denoted $\Delta(\mathcal{I})$, which encapsulate the semantic instruction of a given prompt chunk \mathcal{I} .

This framework establishes a direct connection between the theory of transformer computation and the practice of model control. The derived thought vector $\delta(\mathcal{I})$ provides a theoretical basis for the steering vectors used in activation engineering, explaining why heuristic methods like contrastive averaging are effective. Similarly, the thought matrix $\Delta(\mathcal{I})$ offers a formal justification for low-rank model editing, showing how such modifications can encode complex tasks and instructions, not just simple factual associations. By grounding these empirical techniques in a formal theory, this work bridges the gap between the art of model steering and the science of transformer mechanics, offering a unified perspective on how textual prompts are transmuted into tangible weight updates.

Main Contributions. Our contributions can be summarized as follows:

- We derive a principled method to aggregate transient, token-dependent weight updates into reusable, token-independent *thought vectors* and *thought matrices* that durably encode prompt information.
- We provide a theoretical foundation for heuristic activation steering, demonstrating that the common practice of averaging contrastive activations is equivalent to the least-squares approximation of the optimal thought vector.
- We offer a formal justification for low-rank model editing, showing that the optimal thought matrix naturally emerges as a sum of rank-one updates, aligning with techniques like ROME.
- We empirically validate this framework by transmuting instructions into weights for both algorithmic tasks and knowledge injection, achieving performance comparable to full context prompting in some cases.

1.1 Related work

Our work provides a unified theoretical framework that explains and connects two prominent families of empirical methods for controlling large language models at inference time: activation steering with vectors and direct model editing with matrices. Recent literature suggests these methods operate on a "parametric continuum," where information transitions from volatile prompts to transient activation vectors, and finally to rigid model weights.

Activation Steering with Vectors. One of the most popular methods for guiding a model’s behavior is *activation steering*, which involves adding a "steering vector" to the residual stream activations within each transformer block (Subramani et al., 2022). While these vectors can be learned, they are commonly derived using a simple and effective heuristic: computing the difference between the model’s average activations on a set of "positive" and "negative" prompts (Rimsky et al., 2024). This core idea of using contrastive or averaged activations has been refined and extended in various ways. For instance, some methods use linear probes on the space of contrastive activations to find steering vectors (Li et al., 2023), while others extract them from the principal component of the contrastive embedding differences (Zou et al., 2023).

The most similar vectors to our proposed thought vectors are those computed by simple averaging over contrastive samples (Turner et al., 2025; Chen et al., 2025a), a method shown to be highly reliable in recent benchmarks (Im and Li, 2025). This concept has also been generalized to capture entire tasks, with "function vectors" (Todd et al., 2024) and "task vectors" derived from contrastive prompts (Hendel et al., 2023). Building on this, (Chen et al., 2025a) introduced "persona vectors" to monitor and control high-level character traits, demonstrating that complex behavioral personas can be isolated as single directions. Similarly, Liu et al. (2024) proposed "in-context vectors" to condense demonstrations into a latent steering vector. More recently, Saglam et al. (2025) demonstrated that

these task vectors are modality-independent, confirming they represent functional encodings rather than lexical patterns. Additionally, Li et al. (2025) introduced "implicit in-context learning", proving that demonstration examples can be compressed into a single "context vector" that shifts the model's behavior without processing tokens, validating the transmutation hypothesis.

While heuristic vector addition is effective, Chalnev et al. (2024) utilizes Sparse Autoencoders (SAEs) to target specific features for "surgical" steering. This approach builds directly on the foundational work of Bricken et al. (2023) and Templeton et al. (2024), who demonstrated that SAEs can decompose dense activations into interpretable features which, when clamped, robustly steer model behavior (e.g., the "Golden Gate Claude" experiment). Despite their success, benchmarks show that the performance of vector-based steering methods is not always fully reliable (Tan et al., 2024; Pres et al., 2024), suggesting that vector addition alone may be an incomplete representation of an instruction's full effect (Brumley et al., 2024; Yang et al., 2025a).

Model Editing with Matrices. A parallel line of research focuses on *model editing* through direct modification of a model's weight matrices. These techniques often target the feed-forward layers (FFNs), which have been hypothesized to function as key-value memories storing factual information (Geva et al., 2021). Chen et al. (2025b) refine this view, identifying FFNs as the locus of static distributional associations, while attention layers handle dynamic reasoning. Rather than adding to activations, methods like ROME (Meng et al., 2022) and MEND (Mitchell et al., 2022) apply low-rank updates to the weight matrices to permanently alter knowledge. The formal structure of these matrix edits bears a strong resemblance to our proposed thought matrices. This technique extends to safety controls (Wei et al., 2024) and toxicity reduction (Uppaal et al., 2024).

Recent work explicitly links steering concepts to weight editing. Gur-Arieh et al. (2025) introduced PISCES, which uses SAEs to identify concept directions (similar to steering) and then ablates them directly in the FFN parameters. Similarly, Ruzzetti et al. (2025) developed Private Memorization Editing (PME), targeting FFNs to unlearn memorized PII, further confirming that semantic prompts map to specific physical locations in the weights. Finally, Shafran et al. (2025) propose decomposing MLP activations to map these "transmuted" features back to specific neuron combinations.

Bridging Empirical Methods with Theory. A theoretical explanation for why these interventions work has been missing. To our knowledge, no prior work provides a first-principles strategy to condense information from a generic prompt into a reusable weight update for standard transformers. While Chen et al. (2024) demonstrated exact conversion of ICL to weights for linearized attention, their approach requires architectural modifications.

Our work fills this gap by building on the insights of (Dherin et al., 2025), which extends the "ICL as implicit gradient descent" framework of von Oswald et al. (2023), Dai et al. (2023), and Akyürek et al. (2023). While initial work focused on linear regression, Cheng et al. (2024) proved that Transformers implement *functional* gradient descent to learn non-linear functions. We prove that the effect of a prompt on a standard transformer can be replicated by vector and matrix updates. This aligns with the "task vector" emergence studies of Yang et al. (2025b), but provides the explicit mapping mechanism. Our contribution is to show how these transient, token-specific updates can be aggregated into token-independent *thought patches*, transmuting prompts into durable weights.

2 Token Patches

This section recalls the theory developed in (Dherin et al., 2025). Their work proved that the output of a single transformer block for a prompt $C = [I, x_1, \dots, x_n]$ is equivalent to the output for a shortened prompt $C \setminus I = [x_1, \dots, x_n]$, provided its original feedforward weights are modified for each input token.

We call these token-specific modifications *token patches*. They consist of a vector and a matrix component that must be computed for each token. In essence, the computational effect of the context chunk I can be perfectly replicated by applying these per-token patches to the weights while processing the prompt without I .

2.1 Background

Let's recall the core theorem from (Dherin et al., 2025). A standard transformer block can be described as:

$$T(C, x) = \tilde{W}g_\theta(WA(C, x) + b) + \tilde{b} + A(C, x)$$

where $A(C, x)$ is the output of the self-attention layer for token x within prompt C , and $g_\theta(z)$ is a feedforward network (possibly reduced to a single activation). The authors proved it is possible to find token-dependent weight updates for the last-layer bias and the first-layer weight matrix of the form:

$$b_x(I) = \tilde{b} + \delta_x(I) \quad (1)$$

$$W_x(I) = W + \Delta_x(I) \quad (2)$$

such that removing a context chunk $I \subset C$ from the prompt is equivalent to modifying the weights:

$$T_{W, \tilde{b}}(C, x) = T_{W_x(I), b_x(I)}(C \setminus I, x).$$

The weight updates $\delta_x(I)$ and $\Delta_x(I)$ are the *token patches*. They are given by:

$$\delta_x(I) = A(C, x) - A(C \setminus I, x) \quad (3)$$

$$\Delta_x(I) = \frac{W\delta_x(I)a_x^T}{\|a_x\|^2} \quad (4)$$

where $a_x = A(C \setminus I, x)$ is the attention output for token x in the absence of context I . The primary limitation of this finding, which we address in this paper, is that these patches must be recomputed for each token.

The case of a stack of transformer blocks is handled trivially by starting the implicit update at a given layer and patching the subsequent layers using activations from the previously patched layers (as described, for instance, in Dherin et al. (2025); Goldwaser et al. (2025); Innocenti and Achour (2025)). In particular, Goldwaser et al. (2025) extends these explicit updates to most modern variants of the transformer block including the Gemma block used in 4.

3 From Token Patches to Thought Patches

The token patches $\delta_x(I)$ and $\Delta_x(I)$ depend on the specific token x being processed. This dependency prevents them from being used to store the information from a prompt chunk I in a fixed, reusable form; they would need to be recomputed for every generated token, which is impractical. In this section, we introduce a method to create a single, token-independent *thought patch* that durably encodes the prompt's information into the model's weights.

3.1 Defining Thought Patches

Our goal is to find a single *thought vector* $\delta(I)$ and a single *thought matrix* $\Delta(I)$ that effectively replace the entire collection of token-dependent patches for a given context I .

Consider the activation of a token x_i following a prompt chunk I . This activation, which we'll call x'_i , can be perfectly replicated by removing I and applying the specific token patch (δ_i, Δ_i) to the weights:

$$x'_i = \tilde{W}g_\theta((W + \Delta_i)a_i + b) + (\tilde{b} + \delta_i) + a_i$$

where $a_i = A(x_1, \dots, x_i)$ is the attention output without the context I ,

Ideally, we want to find a single, constant thought patch $(\delta(I), \Delta(I))$ that produces an output y'_i that is identical to x'_i for *any* possible completion of the prompt:

$$y'_i = \tilde{W}g_\theta((W + \Delta(I))a_i + b) + (\tilde{b} + \delta(I)) + a_i$$

However, a single patch that is exact for all possible token sequences may not exist. We therefore seek a close approximation.

3.2 Approximating Thought Patches

A practical approach is to find the thought patch that minimizes the error between its output and the output of the true token patches across a collection of representative examples. Instead of tackling the complex activation error directly, we can simplify the problem by minimizing the error for the vector and matrix components independently.

3.3 Approximating the Thought Vector

For a given collection of prompts, we can find the optimal thought vector by minimizing the squared error against all the individual token vectors (δ_i) derived from that collection. The solution to this minimization problem is simply the mean of all the token vectors:

$$\delta(I) := \frac{1}{n} \sum_{i=1}^n \delta_i$$

3.4 Approximating the Thought Matrix

Similarly, we approximate the thought matrix by finding the matrix M that best satisfies the token patch equation across all examples in our collection. This involves solving the following minimization problem:

$$\min_M \sum_{i=1}^n \|Ma_i - \Delta_i a_i\|^2$$

where $\Delta_i = \frac{W\delta_i a_i^T}{\|a_i\|^2}$ is the token matrix for a given example.

(The index i in the sum above runs over all tokens of all completions $[I, \dots]$ of I in our collection.)

The following theorem gives the solution of this optimization problem:

Theorem 3.1. *Consider n vectors a_1, \dots, a_n in \mathbb{R}^d with which we form the operators $\Delta_i = \frac{W\delta_i a_i^T}{\|a_i\|^2}$ where the $\delta_i \in \mathbb{R}^d$ are fixed vectors. Then the following minimization problem over the space of $d \times d$ matrices*

$$\Delta(I) = \operatorname{argmin}_M \sum_{i=1}^n \|Ma_i - W\delta_i\|^2 \tag{5}$$

has a unique solution if and only if the operator $Z = \sum_{i=1}^n a_i a_i^T$ is invertible. In this case the minimum is reached by

$$\Delta(I) = \left(\sum_{i=1}^n W\delta_i a_i^T \right) Z^{-1} \tag{6}$$

which is a global minimum.

We give a rigorous proof of this theorem in Appendix C.

Now the inverse of Z is computationally difficult to calculate in general. In Appendix C.1, we show that a practical simplification arises if we assume that vectors a_i are spherically distributed for instance. In this case, Z is proportional to the identity matrix:

$$\Delta(I) := \lambda \sum_{i=1}^n W\delta_i a_i^T$$

Here, λ is a tunable hyperparameter.

While we do not require this approximation in our implementation (see Section 4)—as computing $\Delta(I)$ with a general least-squares solver is sufficient and obviates the need to tune λ —the closed-form expressions for $\delta(I)$ and $\Delta(I)$ are of independent interest. They relate directly to the theory of steering vectors and low-rank factual editing, as detailed in the following section.

3.5 Theoretical Foundation for Heuristic Model Editing

The approximation formulas derived above provide a formal, first-principles explanation for the success of several popular, yet heuristic, model control techniques found in the literature.

Our formula for the *thought vector*, $\delta(I) := \frac{1}{n} \sum \delta_i$, serves as a direct theoretical analogue to the methods used to create steering vectors (Subramani et al., 2022), function vectors (Todd et al., 2024), and task vectors (Hendel et al., 2023). These methods typically compute a direction by averaging the activations from contrastive prompts (e.g., positive vs. negative examples). Our theory provides a reason for this: the token vector δ_i is precisely the difference in the attention block’s output with and without the context, $A(C, x_i) - A(C \setminus I, x_i)$. Therefore, the common heuristic of averaging contrastive activations (Turner et al., 2025) is not arbitrary, but is in fact the correct least-squares approximation for a single, token-independent vector that captures the prompt’s instructional content.

Furthermore, our approximation for the *thought matrix*, $\Delta(I) := \lambda \sum W \delta_i a_i^T$, explains the effectiveness of low-rank matrix editing. The formula expresses the thought matrix as a sum of *rank-one matrices*, as each term $\delta_i a_i^T$ is an outer product. This provides a theoretical justification for why low-rank updates are a natural way to modify model behavior. In particular, methods like ROME (Meng et al., 2022), which use targeted rank-one edits to modify factual knowledge, are employing a mathematical structure that our theory identifies as fundamental to how prompt information is encoded. Our derivation suggests that these empirical methods have converged on a technique that is native to the transformer architecture for associating an input direction (a_i) with a corresponding output modification (δ_i).

4 Experimentation

In this section, we empirically validate our approach, demonstrating that the approximated thought patches can specialize a large language model for specific tasks. We accomplish this by directly editing the model’s parameters using our backpropagation-free method, effectively encoding a task instruction into the weights. While a direct implementation (with a least-square solver) of the optimization outlined in Theorem 3.1 achieves near parity with context for prompt describing generic tasks (see Table 1 and Table 2), we need to introduce a modification to deal with context containing new data (see Appendix A).

4.1 The Thought Patching Algorithm

To transmute a specific instruction I into model weights, we employ an iterative layer-wise alignment procedure detailed in Algorithm 1. Our method for computing and applying the thought patches is detailed in Algorithm 1, which is written for a vanilla transformer block. We detail in Appendix A the specific modifications needed for the Gemma architecture. Namely different architectures require slightly different token-patches as shown in (Goldwaser et al., 2025) and (Innocenti and Achour, 2025) for example, which influences the actual form of the thought patch.

The core intuition of our procedure is to align the internal representations of the model processing a raw input x with those of the model processing the instructed input $[I, x]$. We assume a dataset \mathcal{D} of task completions compatible with the instruction I (e.g., if I is “Sum the numbers”, the completions in \mathcal{D} contains sequences like “Input: 3 4 7 Output: 14”).

The algorithm proceeds by iterating through the dataset. For each example, we perform two forward passes:

1. **Contextual Pass (Target):** We run the vanilla model on the full prompt $[I, x_1, \dots, x_n]$. This generates the “ground truth” attention outputs A_l at every layer l , which represent the model’s state when explicitly attending to the instruction.
2. **Non-Contextual Pass (Approximation):** We run the model on the input $[x_1, \dots, x_n]$ *without* the instruction I . Crucially, this pass uses the *currently patched* weights, and is rerun for each layer during patching.

For each layer l , we compute the discrepancy between the target attention output A_l and the current uninstructed output a_l , denoted as $dz_l = A_l - a_l$. We then derive the local thought patch that best bridges this gap. The thought vector update db_l is computed as the mean of these discrepancies,

mirroring the contrastive averaging heuristic. The thought matrix update dW_l is obtained by solving the least-squares minimization problem defined in Theorem 3.1:

$$dW_l = \operatorname{argmin}_M \|Ma_l - W_l d\mathbf{z}_l\|^2.$$

These updates are applied to the model’s parameters, specifically the MLP input projection and output bias.

In Appendix A, we detail the modification needed for a more complex transformer architecture like that of Gemma following the same corrections to the exact token-patches outlined in Goldwaser et al. (2025).

4.2 Enhancing the Algorithm

In this section, we introduce three standard optimization strategies—learning rate schedules, batching, and regularization—to refine the thought patching process. These enhancements improve the stability of the updates and allow the algorithm to generalize better across diverse prompts. These strategies are integrated into the updated procedure detailed in Algorithm 1.

Batching. Rather than computing updates based on a single completion, we can pool the attention values for the completion tokens over a batch of completions to reduce the variance of the thought patch estimation. Let $\mathcal{B} = \{[I, x^{(k)}]\}_{k=1}^B$ be a batch of size B , where $x^{(k)} = [x_{k1}, \dots, x_{kD}]$ are the completion tokens for completion k . Specifically, during both the contextual and non-contextual passes, we record the attention values for all tokens in the batch. These are aligned and stacked into a single tensor \mathbf{A}_l (target attention with context) and \mathbf{a}_l (current attention without context). The least-squares optimization is then performed on these pooled tensors, ensuring the thought matrix dW_l satisfies the projection for the entire batch simultaneously.

Learning Rate. Following a standard practice in model steering (see Chen et al. (2025a) for instance), instead of applying the patch directly, we can scale the update with a tunable step size η (learning rate), gradually encoding the instruction into the weights. For each batch and layer l , the update rule becomes:

$$W_l^{\text{patched}} \leftarrow W_l^{\text{patched}} + \eta \cdot dW_l \quad (7)$$

$$b_l^{\text{patched}} \leftarrow b_l^{\text{patched}} + \eta \cdot db_l \quad (8)$$

Empirically, we found that setting $\eta = 1/N_{\text{batches}}$ (where N_{batches} is the total number of batches) yields consistently stable results.

Regularization. To prevent the thought matrix from overfitting to the specific completions in a batch—which could degrade the model’s general performance—we introduce L_2 regularization (Ridge Regression) to the estimation step. We modify the minimization objective for the thought matrix dW_l as follows:

$$dW_l = \operatorname{argmin}_M \|Ma_l - W_l d\mathbf{z}_l\|_F^2 + \rho \|M\|_F^2 \quad (9)$$

where ρ is the regularization strength and $\|\cdot\|_F$ denotes the Frobenius norm. This encourages minimal weight changes necessary to satisfy the objective.

4.3 Experimental results

All experiments are conducted using the Gemma 3.0 1B Instruction Tuned model (Gemma Team and other authors listed in the paper, 2025). The specific details are collected in Appendix B.

Arithmetic Instruction: Table 1 reports the performance of Algorithm 1 evaluated on simple tasks, such as multiplying or summing numbers. We observe that on these simple tasks performance without the instruction, but with the thought patch applied, matches that of Gemma with the full prompt. In all cases, only 10 examples were required to achieve this parity. Note that the performance of the original model without the instruction is zero. We repeated the experiments 5 times with different patching and evaluation examples to obtain the error bars. Experiment details are in Appendix B.1.

Algorithm 1 Thought Patching

Input: Completions \mathcal{D} of I , Weights W, b , Batch size B , Regularization ρ , Learning Rate η
Initialize: $W^{\text{patched}} \leftarrow W, b^{\text{patched}} \leftarrow b$
// Iterate over dataset in batches
for batch $\mathcal{B} = \{[I, \mathbf{x}^{(k)}]\}_{k=1}^B$ **in** \mathcal{D} **do**
 // **Contextual Pass:** Run orig model with I for $k \in \mathcal{B}$
 // Stack attentions A for all layers across the batch
 $\mathbf{A} = \text{Stack}(\{A_l(I, \mathbf{x}^{(k)}; \text{original})\}_{k,l})$
 for layer l **in** $1, \dots, L$ **do**
 // **Non-Contextual Pass:** Run model *without* I
 // Stack attentions \mathbf{a}_l using current patched weights
 $\mathbf{a}_l = \text{Stack}(\{A_l(\mathbf{x}^{(k)}; \text{patched})\}_k)$
 // Calculate discrepancies (residuals) for the batch
 $\mathbf{dz}_l = \mathbf{A}_l - \mathbf{a}_l$
 // Compute Thought Vector over batch
 $db_l = \text{Mean}(\mathbf{dz}_l)$
 // Compute Thought Matrix via Least Squares
 // Solve: $\min_M \|M\mathbf{a}_l - W_l^{\text{patched}}\mathbf{dz}_l\|^2 + \rho\|M\|^2$
 $dW_l = \text{RidgeSolver}(\mathbf{a}_l \rightarrow W_l^{\text{patched}}\mathbf{dz}_l, \text{reg} = \rho)$
 // Apply scaled updates to the l^{th} layer
 $W_l^{\text{patched}} \leftarrow W_l^{\text{patched}} + \eta \cdot dW_l$
 $b_l^{\text{patched}} \leftarrow b_l^{\text{patched}} + \eta \cdot db_l$
 end for
end for

Table 1: Thought patch performance on arithmetic instruction tasks.

Task (I)	Original model w/ context (Accuracy %)	Patched model w/o context (Accuracy %)
Multiply numbers e.g. 3, 4, 7 \rightarrow 84	100 ± 0.0	100 ± 0.0
Sum numbers e.g. 3, 4, 7 \rightarrow 14	100 ± 0.0	100 ± 0.0

Detoxification: To further test the robustness of our weight-patching method, we apply it to the task of sentence detoxification. This task is significantly harder as it requires the model to transform toxic input into a non-toxic paraphrase of the original input while preserving the original meaning. Table 2 reports the performance of the thought patch computed from an instruction to detoxify a sentence and using demonstrations taken from the ParaDetox dataset from HuggingFace (Logacheva et al., 2022).

We similarly observe that Gemma, without the detoxifying instruction but with the corresponding thought patch, achieves performance comparable to full prompting. Again, only a small number of completions are needed to reach on-par performance. See full experiment details in Appendix B.2.

Table 2: Thought patch performance on detoxification.

Method	Toxicity (%) \downarrow	BERT \uparrow
Toxic Comment	90.53 ± 1.3	-
Neutral Reference	5.62 ± 0.59	-
Original model with context	6.7 ± 0.7	68.09 ± 0.51
Patched model without context	6.22 ± 1.6	62.16 ± 0.25

Translation, Knowledge and Algorithmic Tasks: We also assess the performance of the thought patch on a variety of simple tasks, including translation (French to English, Spanish to English),

stored Knowledge (Country to Capital, Capital to Country) and Algorithmic (First letter of a list), similar to the tasks that were examined in (Hendel et al., 2023). For each of these tasks, the thought patch for the respective instruction I is computed for a small collection of examples; see Appendix B.3 for details.

Table 3 compares the efficacy of the original model with the instruction I to the accuracy of the patched model without the instruction I . As before, over a range of tasks, we observe that the modified Gemma model, without the instruction but with the corresponding thought patch, achieves performance comparable to full prompting in some cases and significantly better than for the original model without context.

Table 3: Thought patch performance on tasks.

Task (I)	Original model w/ context (Accuracy %)	Patched model w/o context (Accuracy %)
French to English e.g. <i>feu</i> → <i>fire</i>	97.37 ± 0.01	92.74 ± 0.25
Spanish to English e.g. <i>fuego</i> → <i>fire</i>	98.4 ± 0.01	94.99 ± 0.43
Country to Capital e.g. France → Paris	79.0 ± 0.21	47.6 ± 1.02
Capital to Country e.g. Paris → France	80.0 ± 0.92	67.2 ± 1.4
List first e.g. a, b, c, d → a	83.25 ± 0.25	31.67 ± 2.3

New Knowledge Integration. While the experiments in Tables 1, 2 and 3 focus on task specialization using knowledge or capabilities already present in the model, Table 4 evaluates the ability of thought patches to encode entirely new information. Specifically, we define the context as a synthetic dictionary of key-value pairs.

We find that the thought patches successfully absorb this new information into the MLP weights, enabling accurate retrieval without the context present. However, performance degrades as the dictionary size increases or when the retrieval templates differ from those used during patch computation (see Table 5). These results highlight a limitation of the current approach: the susceptibility to overfitting on specific prompt structures suggests a need for more robust regularization schemes in future work. As a baseline, the original model achieves zero accuracy without the dictionary in the context. Note that for this task, the thought vector is absorbed into the W_{down} projection rather than the bias, as detailed in A.2. Experiment details are in Appendix B.4.

Table 4: Thought patch performance on new knowledge.

Dictionary Size (I)	Original model w/ context (Accuracy %)	Patched model w/o context (Accuracy %)
$k = 1$	100 ± 0.0	100 ± 0.0
$k = 2$	100 ± 0.0	100 ± 0.0
$k = 4$	100 ± 0.0	100 ± 0.0
$k = 8$	100 ± 0.0	99 ± 1.0
$k = 16$	100 ± 0.0	98 ± 1.0
$k = 32$	100 ± 0.0	91 ± 1.0

5 Conclusion

In this work, we have established a theoretical link between the transient mechanics of transformer inference and permanent model modification. Building on the *token patch* theory of (Dherin et al., 2025), we derived a principled method for aggregating ephemeral weight updates into reusable

thought patches—comprising a thought vector and a thought matrix—that durably encode the semantic instructions of a prompt into the model’s weights.

Our empirical results on Gemma 3 validate that this theoretical framework translates into a practical, data-efficient algorithm for model control. We demonstrated that thought patches can successfully specialize a model for diverse capabilities, achieving performance parity with full-context prompting on tasks ranging from simple arithmetic to language detoxification, often requiring as few as five examples. Furthermore, our experiments with dictionary learning reveal that this technique is not limited to steering existing behaviors; by absorbing thought vectors into projection weights and normalization scales, the model can effectively ingest and retrieve entirely new knowledge not present in its pre-training corpus.

However, our analysis also highlights a current limitation of the method regarding the robustness of these updates. In the case of new knowledge injection, we observed that while the patches encode factual associations effectively for query templates seen during the patching phase, retrieval accuracy degrades when the query phrasing differs significantly from the patching data. This indicates that the current least-squares formulation can overfit to the specific surface form of the completion templates. This finding points to a clear direction for future research: the development of more advanced regularization schemes or data augmentation strategies to ensure that the induced weight updates capture semantic knowledge independent of syntactic structure.

Ultimately, this framework offers a unified physical explanation for the success of heuristic control methods. We showed that the *thought vector* provides the theoretical basis for activation steering (explaining contrastive averaging as a least-squares approximation), while the *thought matrix* justifies low-rank model editing (identifying rank-one updates as the native format of transformer instruction encoding). By bridging the gap between abstract transformer dynamics and tangible weight updates, we provide a robust foundation for the next generation of efficient, mathematically grounded model editing techniques.

References

Nishant Subramani, Nivedita Suresh, and Matthew E. Peters. Extracting latent steering vectors from pretrained language models. In *Findings of the Association for Computational Linguistics: ACL 2022*, pages 566–581, 2022. doi: 10.18653/v1/2022.findings-acl.48. URL <https://aclanthology.org/2022.findings-acl.48/>.

Kenneth Li, Oam Patel, Fernanda Viégas, Hanspeter Pfister, and Martin Wattenberg. Inference-time intervention: Eliciting truthful answers from a language model. *arXiv preprint arXiv:2306.03341*, 2023. NeurIPS 2023 spotlight.

Alexander Matt Turner, Lisa Thiergart, Gavin Leech, David Udell, Juan J Vazquez, Ulisse Mini, and Monte MacDiarmid. Steering language models with activation engineering, 2025. URL <https://openreview.net/forum?id=2XBPdPIcFK>.

Eric Todd, Millicent Li, Arnab Sen Sharma, Aaron Mueller, Byron C Wallace, and David Bau. Function vectors in large language models. In *The Twelfth International Conference on Learning Representations*, 2024. URL <https://openreview.net/forum?id=AwyxtyMwaG>.

Kevin Meng, David Bau, Alex J Andonian, and Yonatan Belinkov. Locating and editing factual associations in GPT. In Alice H. Oh, Alekh Agarwal, Danielle Belgrave, and Kyunghyun Cho, editors, *Advances in Neural Information Processing Systems*, 2022. URL <https://openreview.net/forum?id=-h6WAS6eE4>.

Eric Mitchell, Charles Lin, Antoine Bosselut, Chelsea Finn, and Christopher D Manning. Fast model editing at scale. In *International Conference on Learning Representations*, 2022. URL <https://openreview.net/forum?id=0DcZxeWf0Pt>.

Benoit Dherin, Michael Munn, Hanna Mazzawi, Michael Wunder, and Javier Gonzalvo. Learning without training: The implicit dynamics of in-context learning. *arXiv preprint arXiv:2507.16003*, July 2025. URL <https://arxiv.org/abs/2507.16003>.

Nina Rimsky, Nick Gabrieli, Julian Schulz, Meg Tong, Evan Hubinger, and Alexander Turner. Steering llama 2 via contrastive activation addition. In *Proceedings of the 62nd Annual Meeting of the Association for Computational Linguistics (Volume 1: Long Papers)*, 2024. URL <https://aclanthology.org/2024.acl-long.828/>.

Andy Zou, Long Phan, Sarah Chen, James Campbell, Phillip Guo, Richard Ren, Alexander Pan, Xuwang Yin, Mantas Mazeika, Ann-Kathrin Dombrowski, Shashwat Goel, Nathaniel Li, Michael J. Byun, Zifan Wang, Alex Mallen, Steven Basart, Sanmi Koyejo, Dawn Song, Matt Fredrikson, J. Zico Kolter, and Dan Hendrycks. Representation engineering: A top-down approach to ai transparency, 2023.

Runjin Chen, Andy Ardit, Henry Sleight, Owain Evans, and Jack Lindsey. Persona vectors: Monitoring and controlling character traits in language models, 2025a.

Shawn Im and Yixuan Li. A unified understanding and evaluation of steering methods. *ArXiv*, 2025. URL <https://arxiv.org/abs/2502.02716>.

Roe Hendel, Mor Geva, and Amir Globerson. In-context learning creates task vectors. In *The 2023 Conference on Empirical Methods in Natural Language Processing*, 2023. URL <https://openreview.net/forum?id=QYvF1F19n>.

Sheng Liu, Haotian Ye, Lei Xing, and James Zou. In-context vectors: Making in context learning more effective and controllable through latent space steering. In *Proceedings of the 41st International Conference on Machine Learning*, pages 32287–32307, 2024. URL <https://proceedings.mlr.press/v235/liu24bx.html>.

Baturay Saglam, Xinyang Hu, Zhuoran Yang, Dionysis Kalogerias, and Amin Karbasi. Learning task representations from in-context learning. In *Findings of the Association for Computational Linguistics: ACL 2025*, pages 6634–6663, 2025. URL <https://aclanthology.org/2025.findings-acl.345.pdf>.

Zhuowei Li, Zihao Xu, Ligong Han, Yunhe Gao, Song Wen, Di Liu, Hao Wang, and Dimitris N Metaxas. Implicit in-context learning. In *ICLR*, 2025. URL <https://openreview.net/pdf?id=G7u4ue6ncT>.

Sviatoslav Chalnev, Matthew Siu, and Arthur Conmy. Improving steering vectors by targeting sparse autoencoder features. *arXiv preprint arXiv:2411.02193*, 2024. URL <https://arxiv.org/abs/2411.02193>.

Trenton Bricken, Adly Templeton, Joshua Batson, Brian Chen, Adam Jermyn, Tom Conerly, Nick Turner, Sandipan Kundu, Shan Carter, Tom Henighan, et al. Towards monosemanticity: Decomposing language models with dictionary learning. *Transformer Circuits Thread*, 2023. URL <https://transformer-circuits.pub/2023/monosemantic-features>.

Adly Templeton, Tom Conerly, Jonathan Marcus, Jack Lindsey, Trenton Bricken, Brian Chen, Adam Pearce, Craig Citro, Emmanuel Ameisen, Andy Jones, et al. Scaling monosemanticity: Extracting interpretable features from claude 3 sonnet. *Transformer Circuits Thread*, 2024. URL <https://transformer-circuits.pub/2024/scaling-monosemanticity>.

Daniel Chee Hian Tan, David Chanin, Aengus Lynch, Brooks Paige, Dimitrios Kanoulas, Adrià Garriga-Alonso, and Robert Kirk. Analysing the generalisation and reliability of steering vectors. In *Advances in Neural Information Processing Systems*, volume 37, 2024.

Itamar Pres, Laura Ruis, Ekdeep Singh Lubana, and David Krueger. Towards reliable evaluation of behavior steering interventions in llms. *ArXiv*, abs/2410.17245, 2024. URL <https://arxiv.org/abs/2410.17245>.

Madeline Brumley, Joe Kwon, David Krueger, Dmitrii Krasheninnikov, and Usman Anwar. Comparing bottom-up and top-down steering approaches on in-context learning tasks. *ArXiv*, 2024. URL <https://arxiv.org/abs/2411.07213>.

Liu Yang, Ziqian Lin, Kangwook Lee, Dimitris Papailiopoulos, and Robert Nowak. Task vectors in in-context learning: Emergence, formation, and benefit, 2025a. URL <https://arxiv.org/abs/2501.09240>.

Mor Geva, Roei Schuster, Jonathan Berant, and Omer Levy. Transformer feed-forward layers are key-value memories, 2021. URL <https://arxiv.org/abs/2012.14913>.

Lei Chen, Joan Bruna, and Alberto Bietti. Distributional associations vs in-context reasoning: A study of feed-forward and attention layers. In *Proceedings of the International Conference on Learning Representations (ICLR)*, 2025b. URL <https://arxiv.org/abs/2406.03068>.

Boyi Wei, Kaixuan Huang, Yangsibo Huang, Tinghao Xie, Xiangyu Qi, Mengzhou Xia, Prateek Mittal, Mengdi Wang, and Peter Henderson. Assessing the brittleness of safety alignment via pruning and low-rank modifications. In *ICLR 2024 Workshop on Mathematical and Empirical Understanding of Foundation Models*, 2024. URL <https://openreview.net/forum?id=niBPvgJIHB>.

Rheeya Uppaal, Apratim Dey, Yiting He, Yiqiao Zhong, and Junjie Hu. Model editing as a robust and denoised variant of DPO: A case study on toxicity. In *Neurips Safe Generative AI Workshop 2024*, 2024. URL <https://openreview.net/forum?id=2I821Dypa2>.

Yoav Gur-Arieh, Clara Suslik, Yihuai Hong, Fazl Barez, and Mor Geva. Precise in-parameter concept erasure in large language models. In *Proceedings of the 2025 Conference on Empirical Methods in Natural Language Processing*, 2025. URL <https://arxiv.org/abs/2505.22586>. Introduces PISCES framework.

Elena Sofia Ruzzetti, Giancarlo A Xompero, Davide Venditti, and Fabio Massimo Zanzotto. Private memorization editing: Turning memorization into a defense to strengthen data privacy in large language models. In *Proceedings of the 63rd Annual Meeting of the Association for Computational Linguistics (ACL 2025)*, 2025. URL <https://aclanthology.org/2025.acl-long.810/>.

Or Shafran, Atticus Geiger, and Mor Geva. Decomposing mlp activations into interpretable features via semi-nonnegative matrix factorization. *arXiv preprint arXiv:2506.10920*, 2025. URL <https://arxiv.org/abs/2506.10920>.

Brian K Chen, Tianyang Hu, Hui Jin, Hwee Kuan Lee, and Kenji Kawaguchi. Exact conversion of in-context learning to model weights in linearized-attention transformers. In *Proceedings of the 41st International Conference on Machine Learning*, ICML 2024, 2024.

Johannes von Oswald, Eyvind Niklasson, Ettore Randazzo, João Sacramento, Alexander Mordvintsev, Andrey Zhmoginov, and Max Vladymyrov. Transformers learn in-context by gradient descent. In *Proceedings of the 40th International Conference on Machine Learning*, volume 202, pages 35151–35174, 2023. URL <https://proceedings.mlr.press/v202/von-oswald23a.html>.

Damai Dai, Yutao Sun, Li Dong, Yaru Hao, Shuming Ma, Zhifang Sui, and Furu Wei. Why Can GPT Learn In-Context? Language Models Implicitly Perform Gradient Descent as Meta-Optimizers. In *Findings of the Association for Computational Linguistics: ACL 2023*, pages 4005–4019. Association for Computational Linguistics, 2023.

Ekin Akyürek, Dale Schuurmans, Jacob Andreas, Tengyu Ma, and Denny Zhou. What learning algorithm is in-context learning? investigations with linear models. In *ICLR*, 2023.

Xiang Cheng, Yuxin Chen, and Suvrit Sra. Transformers implement functional gradient descent to learn non-linear functions in context. In *ICML*, pages 8002–8037. PMLR, 2024. URL <https://proceedings.mlr.press/v235/cheng24a.html>.

Liu Yang, Ziqian Lin, Kangwook Lee, Dimitris Papailiopoulos, and Robert Nowak. Task vectors in in-context learning: Emergence, formation, and benefit. In *Proceedings of COLM 2025*, 2025b. URL <https://arxiv.org/abs/2501.09240>.

Adrian Goldwaser, Michael Munn, Javier Gonzalvo, and Benoit Dherin. Equivalence of context and parameter updates in modern transformer blocks, 2025. URL <https://arxiv.org/abs/2511.17864>.

Francesco Innocenti and El Mehdi Achour. A simple generalisation of the implicit dynamics of in-context learning, 2025. URL <https://arxiv.org/abs/2512.11255>.

Gemma Team and other authors listed in the paper. Gemma 3 Technical Report. *arXiv preprint arXiv:2503.19786*, 2025. URL <https://arxiv.org/abs/2503.19786>.

Varvara Logacheva, Daryna Dementieva, Sergey Ustyantsev, Daniil Moskovskiy, David Dale, Irina Krotova, Nikita Semenov, and Alexander Panchenko. ParaDetox: Detoxification with parallel data. In *Proceedings of the 60th Annual Meeting of the Association for Computational Linguistics (Volume 1: Long Papers)*, 2022.

Noam Shazeer. GLU variants improve transformer. *arXiv preprint arXiv:2002.05202*, 2020.

Sheng Liu, Haotian Ye, Lei Xing, and James Zou. In-context vectors: Making in context learning more effective and controllable through latent space steering. *arXiv preprint arXiv:2311.06668*, 2023.

A Algorithm modification for Gemma

This appendix details the specific adaptations required to apply the Thought Patching algorithm to the Gemma 3 architecture (Gemma Team and other authors listed in the paper, 2025), which differs from the vanilla transformer block primarily in its use of RMSNorm and Gated GeLU feed-forward networks.

A.1 Adapting the Thought Matrix for Gated GeLU and Pre-normalization

A standard Gemma block is depicted in Figure 1.

As established in Section 3, the thought vector $\delta(I)$ corresponds to a bias shift in the residual stream and can be computed from the output $A(C, x)$ of the conceptual layer. However, the computation of the thought matrix $\Delta(I)$ requires careful selection of the input activation vector a_l .

In a standard transformer, the MLP input is often the direct output of the attention mechanism (or the residual stream). In Gemma, the input to the Multi-Layer Perceptron (MLP) passes through a normalization layer (RMSNorm) first. Therefore, strictly applying the update to the matrices W_{up} and W_{gate} requires using the activations *after* this normalization. We denote this activation as $\hat{a}_l = \text{RMSNorm}(z_l)$, corresponding to the ‘‘Normalized input’’ point in the computational graph.

Furthermore, the Gemma architecture utilizes a Gated GeLU activation function Shazeer (2020), meaning the first layer of the MLP is split into two distinct projections: an upward projection W_{up} and a gating projection W_{gate} . The activation is computed as:

$$\text{MLP}_{\text{in}}(\hat{a}_l) = (W_{\text{gate}}\hat{a}_l) \odot \sigma(W_{\text{up}}\hat{a}_l) \quad (10)$$

where σ is the activation function (e.g., GeLU) and \odot denotes element-wise multiplication. Consequently, the single thought matrix optimization problem described in Theorem 3.1 must be decoupled into two independent least-squares estimations similarly to (Goldwaser et al., 2025).

For a given layer l , let \hat{a}_l be the stacked normalized activations and \mathbf{dz}_l be the target residual discrepancies. We solve:

$$dW_{l,\text{up}} = \operatorname{argmin}_M \left\| M\hat{a}_l - W_{l,\text{up}}^{\text{patched}} \mathbf{dz}_l \right\|_F^2 + \rho \|M\|_F^2 \quad (11)$$

$$dW_{l,\text{gate}} = \operatorname{argmin}_M \left\| M\hat{a}_l - W_{l,\text{gate}}^{\text{patched}} \mathbf{dz}_l \right\|_F^2 + \rho \|M\|_F^2 \quad (12)$$

This ensures that the thought patch correctly influences both the gating mechanism and the content projection.

A.2 Absorbing the Thought Vector into Weights and Scale

A significant architectural challenge in applying the thought patches to Gemma is the absence of explicit bias parameters in the MLP output layer. While the theoretical framework in Section 3.4 predicts a thought vector update $b^{\text{patched}} = b + \delta(I)$, the Gemma architecture computes the MLP output via a strictly linear projection $W_{l,\text{down}}$:

$$x_{l,\text{out}} = x_{l,\text{in}} + W_{l,\text{down}} h_l \quad (13)$$

where h_l is the hidden state after the Gated GeLU activation for layer l . To implement the affine shift $\delta(I)$ without an architectural modification (i.e., without inserting a new bias tensor), we adopt the projection method proposed by Goldwaser et al. (2025) to absorb the shift directly into W_{down} .

An additional complexity arises from the use of RMSNorm after the MLP in Gemma. To address this, we follow the method from Goldwaser et al. (2025). The objective is to modify W_{down} such that its output effectively includes the shift $\delta(I)$, accounting for the specific scaling characteristics of the layer.

Let d_l and d_l^C denote the output activations of the linear projection $W_{l,\text{down}}$ in the non-contextual and contextual passes, respectively. Let s_l represent the RMSNorm scale parameter for layer l . We first compute a target activation vector, d_l^{goal} , which incorporates the desired thought vector shift adjusted by the layer’s normalization scale:

$$d_l^{\text{goal}} = (\delta(I) \odot s_l) + d_l^C - d_l \quad (14)$$

where \oslash denotes element-wise division. This adjustment ensures that the bias shift aligns correctly with the layer's activation distribution.

To prevent the weight update from destabilizing the model by altering the norm of the MLP output significantly, we impose a magnitude constraint. We construct a normalized target \hat{d}_l^{goal} that preserves the direction of the calculated goal but matches the magnitude of the ground-truth contextual activations:

$$\hat{d}_l^{\text{goal}} = \frac{\|d_l^C\|_2}{\|d_l^{\text{goal}}\|_2} \cdot d_l^{\text{goal}} \quad (15)$$

Finally, we find the optimal update for the projection matrix by solving the least-squares minimization problem over the activations h_l :

$$dW_{l,\text{down}} = \operatorname{argmin}_M \left\| Mh_l - \hat{d}_l^{\text{goal}} \right\|_F^2 + \rho \|M\|_F^2 \quad (16)$$

Although this formulation technically allows for updating the RMSNorm scale s_l to correct residual magnitude discrepancies, we find empirically that updating only the matrix W_{down} and leaving s_l as its original value is sufficient for high-fidelity instruction following and knowledge absorption and helps maintain performance.

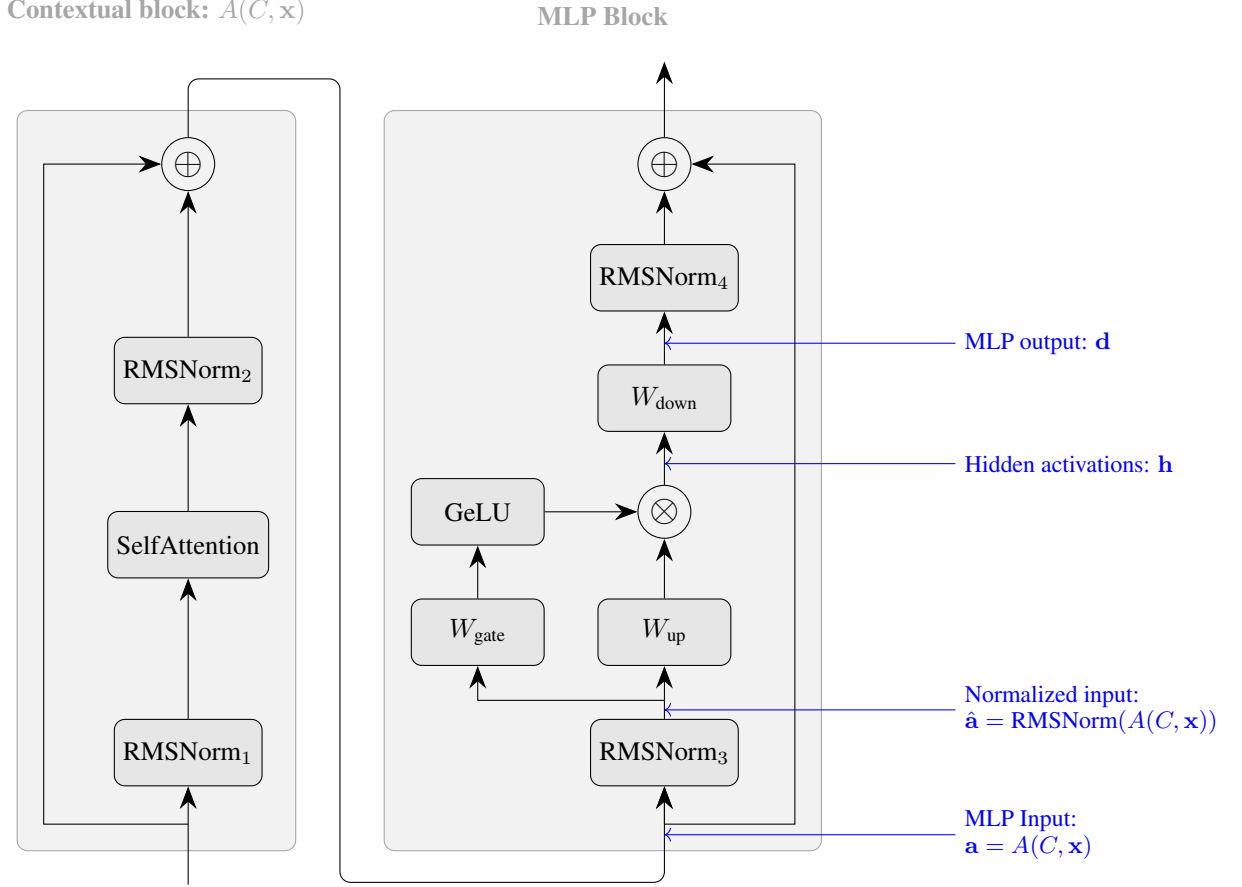


Figure 1: The Gemma block architecture. Note the pre-feedforward and post-feedforward normalization, the split gating mechanism and the lack of a bias parameter, which necessitate the specific algorithm modifications detailed in Appendix A.

B Experiment Details

All experiments were conducted using the Gemma 3.0 1B model Gemma Team and other authors listed in the paper (2025). As noted in the main text, the specific architectural features of Gemma—namely RMSNorm and GeLU gating—necessitate the modifications to Algorithm 1 detailed in Appendix A.

For each experimental task, we record and align the model’s intermediate activations across two distinct pass types:

1. **Contextual Pass (Target):** The model processes the full prompt containing the specific instruction I (the context). This serves as the ground truth for the optimization objective.
2. **Non-Contextual Pass (Approximation):** The model processes only the input data (completion) wrapped in the standard chat template, without the explicit instruction I .

To ensure precise alignment of the hidden states during the least-squares estimation, we include the model’s generated response (the answer) in both passes. This ensures the patch minimizes the divergence between the *instructed* and *uninstructed* processing of the exact same token sequence. The prompt templates are structured as follows:

```
# Contextual Prompt (Target)
<start_of_turn>user
{context}{completion}<end_of_turn>
<start_of_turn>model
{answer}<end_of_turn>

# Non-Contextual Prompt (Approximation)
<start_of_turn>user
{completion}<end_of_turn>
<start_of_turn>model
{answer}<end_of_turn>
```

B.1 Arithmetic and Linguistic Tasks (Table 1)

Arithmetic Experiments. The instruction context I was defined as either “Sum the numbers:” or “Multiply the numbers:”. To establish a rigorous baseline where the unpatched model achieves 100% accuracy with context, we restricted the dataset to operations on three single-digit integers. Representative prompts for the multiplication task are shown below:

```
<start_of_turn>user
Multiply the numbers:
5 9 4<end_of_turn>
<start_of_turn>model
180<end_of_turn>
```

For the non-contextual pass, the line “Multiply the numbers:” is omitted. We constructed the thought patches using a dataset \mathcal{D} of 10 completions per task. We employed a learning rate of $\eta = 0.1$, a batch size of 1, and no regularization ($\rho = 0$). Convergence to 100% accuracy on the training set was observed after 10 steps for both multiplication and summation. We validated the induced thought patches on a held-out test set of 20 randomly regenerated examples at each step, achieving 100% peak test accuracy over the 10 steps for each of 5 random seeds.

B.2 Detoxification (Table 2)

To further test our weight-patching method on more complex semantic steering, we applied it to the task of sentence detoxification. This task requires the model to transform toxic input into a non-toxic paraphrase while preserving the original meaning. For these experiments we used the following contextual instruction

```
Please detoxify the following sentence. Return a single
detoxified statement. Do not provide any commentary or
```

suggestions. Return a single detoxified statement that is a detoxified version of the original sentence but that still has the same semantic meaning as the original. Here is the original toxic sentence:

We used the ParaDetox dataset from HuggingFace, a high-quality corpus containing pairs of toxic comments and their detoxified counterparts and is designed specifically for this style transfer task. We used only 10 examples from the ParaDetox training split to compute the weight update with one training step and a learning rate $\eta = 1.0$ and no regularization $\rho = 0$. For evaluation we compared the original model with the given detoxification instruction against the patched model with no detoxification instruction; i.e., given only the toxic sentence. For each of these, we measured the toxicity of the model output, with a lower score indicating less toxicity.

We measured the toxicity levels of the model’s outputs using a pre-trained BERT-based toxicity classifier (specifically, the `unitary/toxic-bert` model). This evaluator provides a probability score across multiple categories, including “Toxic”, “Severely Toxic”, “Obscene”, “Threat”, “Insult” and “Identity Hate”. In Table 2 we report the average “Toxic” score for 100 examples drawn from the ParaDetox test set.

A primary challenge in detoxification is ensuring that the “detoxified” output does not lose the underlying intent or information of the original sentence. To also measure this, we employed a BERT-based semantic similarity metric, as in Liu et al. (2023). By comparing the output of the original model and the patched model against the ground-truth human references in the ParaDetox test set, we can quantify how well the model “internalized” the detoxification logic without sacrificing semantic accuracy, with a higher BERT score indicates a closer semantic relationship.

B.3 Translation, Knowledge and Algorithmic Tasks (Table 3)

We also explored the efficacy of our thought patches for simple tasks such as Translation (French or Spanish to English), Knowledge (Country to Capital and Capital to Country) and Algorithmic Tasks (determine the first letter of a string).

Translation Experiment. We evaluated the capability of thought patches to induce translation behavior from a foreign source language (e.g., French or Spanish) to English. We focus only on dictionary translation of specific words and not phrases. For French-to-English we use the context I to be

Translate the following word from French
to English. Return only a single English
word that is the translation of the
French word {foreign_source_word}.

Similarly, for Spanish-to-English we use the context

Translate the following word from
Spanish to English. Return only a single
English word that is the translation of
the Spanish word {foreign_source_word}.

For the non-contextual pass, the instruction to translate is omitted and only the French (or Spanish) word is provided to the model. We computed the thought patches using a dataset of 10 completions using a learning rate of $\eta = 1.0$ and no regularization, $\rho = 0.0$. We validated the original model and the patched model on a hold out set of 100 French (or Spanish) words and compared the provided translation against the dictionary English reference.

Because there is some variability in translation, meaning a model might produce a valid translation that does not perfectly match the literal string of a dictionary reference, we evaluate performance based on semantic similarity rather than exact word matching. To do this, we use a pre-trained BERT model to convert both the model’s output and the gold-standard English dictionary reference into high-dimensional feature embeddings and then calculate the similarity between these two vectors. This BERT-based score ranges from 0 to 1, where a score of 1.0 represents a perfect semantic match.

This approach allows us to capture how well the patched model preserves the meaning of the intended translation, even if the specific word choice varies slightly.

Prior Knowledge For this task, the contextual prompt asks the model to return the capital city when provided a country or, vice versa, return the country when given a capital city. The instruction prompt (resp.) that we used to compute the thought patch over demonstrations is

Give me the capital of the following country. Return only a single city that is the capital of the country

and

Give me the country of the following capital city. Return only a single country that is the country of the capital

For these experiments we used 5 demonstration examples with a learning rate of 1.0 and no regularization $\rho = 0.0$. Since knowledge of a capital city or country is binary (i.e., either the response is correct or not), in Table 3 we report the accuracy of the original model with the given context and country (resp. capital) against the accuracy of the patched model given only the country (resp. capital). We compute the accuracy over 100 examples of pairs of country and capitals that were not used to compute the thought patch.

B.4 New Knowledge Integration (Table 4)

Dictionary Task. We investigated the capacity of thought patches to encode entirely new factual associations not present in the pre-training corpus. The context I consisted of a synthetic dictionary defining key-value pairs (e.g., “ $k_1 \rightarrow v_1$ ”). We evaluated the patched model’s accuracy on retrieval queries without the dictionary present in the context.

To prevent the injection of new knowledge from destabilizing the model’s activations, we utilized the projection and scaling techniques described in Appendix A. Specifically, the thought vector was absorbed into the output projection W_{down} . We report retrieval accuracy for dictionary sizes $k \in \{1, 2, 4, 8, 16, 32\}$ below. For larger dictionaries ($k \geq 16$), we had to perform a rank reduction by keeping the 40 principal components of the matrices returned by the least-square solver. The keys and values in the dictionaries were randomly generated numbers from 0 to 100. In all cases, we batched all completions and computed the patches in one step with a learning rate of $\eta = 1$, a regularization rate of $\rho = 0.5$ for the L2 penalty on the least-square. The context was the data of the dictionary assignment $M=\{\dots\}$, while the completion was one of the following query versions, chosen randomly:

Answer with one word, \
 - the value of {dict_name}["{key}"] is
 - {dict_name}["{key}"] equals
 - the value of {dict_name} \
 for key "{key}" is

The answer was simply the actual value corresponding to the query, yielding contextual prompts of the form:

```
<start_of_turn>user
M={"1": "50", "38": "24"}
Answer with one word,\  

the value of M["1"] is<end_of_turn>
<start_of_turn>model
50<end_of_turn>
```

We use the heuristic formula $n * k$ to estimate the number of completions needed with $n = 3$ referring to the number of query versions used.

We observe also a significant loss of performance when the retrieval queries used to evaluate the patch are different from the ones used to compute the patch, which points to a need to properly tune

the regularization parameter, and constitute a limitation of this work. Table 5 reports the accuracy when we use the following queries to evaluate rather that the ones mentioned above to compute the patch (the errors were computed over 5 random seeds):

Answer with one word, \

- what value corresponds \
- to key "{key}" in {dict_name}?
- retrieve the content \
- of {dict_name}["{key}"].
- what is stored in {dict_name}
- under the key "{key}"?

Table 5: Thought patch performance on new knowledge evaluated on different queries.

Dict. Size (I)	Accuracy patched model same queries (%)	Accuracy patched model different queries (%)
k = 1	100 ± 0.0	100 ± 0.0
k = 2	100 ± 0.0	100 ± 0.0
k = 4	100 ± 0.0	83.3 ± 4.0
k = 8	99 ± 1.0	79.1 ± 6.7
k = 16	98 ± 1.0	53.0 ± 6.6
k = 32	91 ± 1.0	42.7 ± 7.8

C Thought Matrix Estimation Theorem

In Section 3.4, we introduced the thought matrix representing the thought expressed in a chunk I of a prompt as the matrix $\Delta(I)$ that minimizes the errors $\|\Delta(I)a_i - \Delta_i a_i\|^2$ for all completions $[I, x_1, \dots, x_i]$ formed by all the partial prompts in our collection of prompts, and where

$$\Delta_i = \frac{\delta_i a_i^T}{\|a_i\|^2}$$

is the token matrix for token x_i with attention a_i in the absence of I and δ_i the corresponding thought vector.

In this section, we give a rigorous result that shows that this minimizer exists and is unique if and only if the following operator is invertible

$$Z = \sum_{i=1}^n a_i a_i^T.$$

In Appendix C.1, we provide a list of settings for this invertibility to happen. The proof for the invertibility conditions are in Appendix D given in the form of a series of generic lemma for low-rank operators.

Theorem C.1. *Consider n vectors y_1, \dots, y_n in \mathbb{R}^d with which we form the operators $\Delta_i = \frac{\delta_i y_i^T}{\|y_i\|^2}$ where the $\delta_i \in \mathbb{R}^d$ are fixed vectors. Then the following minimization problem over the space of $d \times d$ matrices*

$$\min_M \sum_{i=1}^n \|My_i - \Delta_i y_i\|^2, \quad (17)$$

has a unique solution if and only if the operator $Z = \sum_{i=1}^n y_i y_i^T$ is invertible. In this case the minimum is reached by

$$M = \left(\sum_{i=1}^n \delta_i y_i^T \right) Z^{-1}, \quad (18)$$

which is a global minimum.

Proof. The minimum is achieved at a critical point of the error function

$$L(M) = \sum_{i=1}^n \|My_i - \Delta_i y_i\|^2, \quad (19)$$

which is a point at which its gradient vanishes, i.e., $\nabla_M L(M) = 0$. Since the gradient of L is given by

$$\nabla_M L(M) = 2 \sum_{i=1}^n (My_i - \Delta_i y_i) y_i^T. \quad (20)$$

then M is a critical point if and only if:

$$\sum_{i=1}^n (My_i - \Delta_i y_i) y_i^T = 0, \quad (21)$$

which we can rewrite as

$$M \left(\sum_{i=1}^n y_i y_i^T \right) = \sum_{i=1}^n \Delta_i y_i y_i^T. \quad (22)$$

Now since for the operator Δ_i , we have the following property

$$\Delta_i y_i y_i^T = \frac{\delta_i (y_i^T y_i) y_i^T}{\|y_i\|^2} = \delta_i y_i^T \quad (23)$$

then M is a critical point of L if and only if

$$M Z = \sum_{i=1}^n \delta_i y_i^T. \quad (24)$$

Now if Z is invertible, we obtain that the critical exists and is unique given by

$$M = \left(\sum_{i=1}^n \delta_i y_i^T \right) Z^{-1}. \quad (25)$$

To prove the converse, suppose by contradiction that M exists and is unique but that Z is not invertible. Since Z is not invertible, its image $V = \text{Image}(Z)$ is a strick subspace of \mathbb{R}^d . Consider an operator A that is the identity on V but move the orthogonal space V^T around. Then $MAZ = MZ$ but $M \neq MA$ since the two operators have a different action on V^T . This means that for the new operator $M' = MA$, we also have that

$$M'Z = \sum_{i=1}^n \delta_i y_i^T, \quad (26)$$

which means that it is a critical point of L_M and $M' \neq M$, contradicting the uniqueness assumption.

Observe at this point, that to fully complete the proof, we should ensure that M is a global minimum, not just a critical point. Under our assumption that Z is invertible, we just showed that $L(M)$ has a single critical point. Since $L(M)$ is positive and goes to infinity as M becomes large, then this single critical point can only be a minima. Since there is only one minima, it is a global minima. \square

From the theorem above, we see that the matrix M that minimizes

$$\min_M \frac{1}{n} \sum_{i=1}^n \|My_i - \Delta_i y_i\|^2, \quad (27)$$

crucially depends on the forms of the inverse of Z . We list here a few cases, where Z can be explicitly computed.

C.1 Invertibility Conditions for Z

We now gives conditions on the vector y_1, \dots, y_n for the matrix

$$Z = \sum_i y_i y_i^T$$

in Theorem C.1 to be invertible. These settings are certainly not the only ones, but they are easy enough to describe analytically. The proof of our statements are in Appendix D:

1. Z is invertible if and only if $y_1, \dots, y_n \in \mathbb{R}^d$ span the whole vector space (see Lemma D.2); however, in this case the form of the inverse is difficult to compute explicitly.
2. When y_1, \dots, y_n is a basis of the space (which implies that $n = d$), then the inverse takes the form

$$Z = \sum_i \omega_i \omega_i^T,$$

where the vectors ω_i are the rows of Y^{-1} . This means that $Z^{-1} = (Y^T)^{-1} Y^{-1}$ and that the ω_i are the co-vector basis associated with the basis y_1, \dots, y_n (i.e. $\omega_i^T y_j = \delta_{ij}$ where δ_{ij} is the Kronecker delta. (See Lemma D.3.)

3. When y_1, \dots, y_n is an orthonormal basis ($n = d$) of the space

$$Z^{-1} = I.$$

(See Lemma D.4.)

4. When y_1, \dots, y_n are vectors independently sampled from a spherical distribution, then for n large enough

$$Z^{-1} = \frac{1}{\sigma^2 n} I,$$

where σ^2 is the distribution variance. (See Lemma D.7.)

C.2 Getting an approximation of M when Z is not invertible

We are seeking operators M such that when applied to the y_i 's they give back the δ_i 's as closely as possible. That is, we are looking to minimize the following linear regression problem:

$$\min_M \sum_i \|My_i - \delta_i\|^2 \quad (28)$$

In fact, the proof of Theorem C.1 shows us that any matrix satisfying the following equation is an optimum:

$$MZ = \delta Y^T, \quad (29)$$

where $Z = YY^T$. The solution is clear when Z is invertible and given in Theorem C.1, but in practice it may not be. In this case, we can always add a small diagonal matrix $\epsilon = \text{diag}(\epsilon_1, \dots, \epsilon_d)$ to Z to render it invertible: $Z_e = e + Z = e(1 + e^{-1}Z)$, whose inverse can be approximated as

$$Z_e^{-1} = (1 + e^{-1}Z)^{-1}e^{-1} \simeq (1 - e^{-1}Z)e^{-1} = c - cZc, \quad (30)$$

where in the last equation we set $c = \text{diag}(c_1, \dots, c_d)$ to be the inverse of ϵ (i.e. $c_i = 1/\epsilon_i$). Now, we can solve $MZ_e = \delta Y^T$ using this approximated inverse, yielding:

$$M = \delta Y^T(c - cZ^2) = \delta Y^T c - c\delta Y^T c. \quad (31)$$

In particular, if we take c to be a constant λ time the identity, we obtain the following approximation:

$$M = \lambda \sum_{i=1}^n \delta_i y_i^T - \lambda^2 \sum_{i,j=1}^n \langle y_i, y_j \rangle \delta_i y_j^T, \quad (32)$$

where we will understand λ as a tunable hyper-parameter.

D Useful properties of low-rank operators

Consider linear a application $A : \mathbb{R}^d \rightarrow \mathbb{R}^d$ represented by a matrix

$$A = \sum_{i=1}^r v_i w_i^T, \quad (33)$$

where v_i, w_i are column vectors in \mathbb{R}^d with $r < d$. If we write V to be the matrix whose columns are the v_i 's and W the matrix whose columns are the w_i 's we can write A in matrix notation as

$$A = VW^T. \quad (34)$$

These matrices represent the general form of the low-rank operators implementing the thought matrices we have been dealing with in this paper. In the rest of this section, we prove a number of basic lemmas outlining properties that are important for this study. First of all let us start by determining the actual rank, image, and kernel of these operators:

D.1 Image, kernel, and rank

Lemma D.1. *Consider a low-rank operator with matrix given by*

$$A = \sum_{i=1}^r v_i w_i^T$$

as above. Let us denote by $V = \text{span}\{v_i\}$ and $W = \text{span}\{w_i\}$ the linear subspaces spanned by the vectors v_i and w_i respectively for $i = 1, \dots, r$. Then the rank of A is bounded by r . More precisely, we have that

$$\text{rank}(A) \leq \min\{\dim V, \dim W\} \leq r. \quad (35)$$

and that

$$\text{image}(A) \subset V \quad \text{and} \quad W^\perp \subset \text{kernel}(A). \quad (36)$$

Moreover when the v_i 's and the w_i 's are independent then we have equality everywhere:

$$\text{rank}(A) = r, \quad \text{image}(A) = V, \quad \text{kernel}(A) = W^\perp. \quad (37)$$

Proof. First of all, we trivially have that $\text{image}(A) \subset V$ and $W^\perp \subset \text{kernel}(A)$. Now, since $\text{rank}(A) = \dim \text{image}(A)$ by definition, we immediately have the $\text{rank}(A) \leq \dim V$. Now consider the kernel-image relation, that is, that $\dim \text{image}(A) + \dim \text{kernel}(A) = d$, where d is the dimension of the space. Combining this relation with $W^\perp \subset \text{kernel}(A)$, we obtain the inequality

$$\text{rank}(A) + \dim W^\perp \leq d. \quad (38)$$

Now since $\dim W^\perp = d - \dim W$, we obtain from the inequality above that

$$\text{rank}(A) + d - \dim W \leq d, \quad (39)$$

which yields that $\text{rank}(A) \leq \dim W$, proving the first part of the statement.

Now, let us consider the case when the v_i 's and the w_i 's are independent. By independence we immediately obtain that $\dim V = \dim W = r$, and therefore we get that $\text{rank}(A) = r$. Since $\text{image}(A) \subset V$ and both spaces have the same dimension r , they must coincide: $\text{image}(A) = V$

As for the kernel, to show that $\text{kernel}(A) = W^\perp$, we only need to show the other inclusion direction: $\text{kernel}(A) \subset W^\perp$. Let us take a vector x in the kernel of A . Then we get that

$$0 = Av = \sum_{i=1}^r v_i w_i^T x = \sum_{i=1}^r \langle w_i, x \rangle w_i. \quad (40)$$

By independence of the w_i 's, we obtain that $\langle w_i, x \rangle = 0$ for $i = 1, \dots, r$. This exactly means that x is orthogonal to W , that is, $x \in W^\perp$. Thus $\text{kernel}(A) = W^\perp$.

□

D.2 Independence, span, and basis

Let us now focus on the invertibility of operators of the form $Z = \sum_i y_i y_i^T$. The next lemma shows that the y_i 's must span the vector space:

Lemma D.2. *Let $y_1, \dots, y_n \in \mathbb{R}^d$ and consider the linear map*

$$Z = \sum_{i=1}^n y_i y_i^T. \quad (41)$$

Then Z is invertible if and only if the y_i 's span the vector space \mathbb{R}^d .

Proof. Suppose that the y_i 's span the whole vector space \mathbb{R}^d . By Lemma D.1, we have that $\text{image}(Z) = \text{span}(y_1, \dots, y_n) = \mathbb{R}^n$, which means that Z is subjective. An operator $Z : \mathbb{R}^d \rightarrow \mathbb{R}^d$ defined on the same space can be subjective if and only if it is bijective, i.e., invertible.

To prove the converse, suppose that Z is invertible. We need to prove that any vector $v \in \mathbb{R}^d$ can be written as a linear combination of the y_i 's. Since Z is invertible, let us denote by $a = Z^{-1}v$ the inverse image of v by Z . Now we have that

$$v = Za = \left(\sum_{i=1}^n y_i y_i^T \right) a = \sum_{i=1}^n \alpha_i y_i, \quad (42)$$

where $\alpha_i = y_i^T a$, which finishes proving the converse.

□

Lemma D.3. *Let $y_1, \dots, y_d \in \mathbb{R}^d$ be a basis, and consider the linear map*

$$Z = \sum_{i=1}^n y_i y_i^T. \quad (43)$$

Then Z is invertible with inverse given by

$$Z^{-1} = (Y^{-1})^T Y^{-1} = \sum_{j=1}^n \omega_j \omega_j^T, \quad (44)$$

where Y is the matrix with columns y_1, \dots, y_n , and the ω_j 's are the columns of the matrix $(Y^{-1})^T$.

Proof. If y_1, \dots, y_d is a basis, it means that these vectors are independent. This means that the determinant of the matrix Y with the y_i 's as columns is non zero: $\det Y \neq 0$. This means that it is invertible, and so is its transpose. Now, since $Z = YY^T$, it is easy to verify that

$$(Y^T)^{-1}Y^{-1}Z = Z(Y^T)^{-1}Y^{-1} = I. \quad (45)$$

Now that we have established that $Z^{-1} = (Y^{-1})^T Y^{-1}$, setting $\Omega = (Y^{-1})^T$, we see that $Z^{-1} = \Omega \Omega^T$, concluding that $Z^{-1} = \sum_{i=1}^n \omega_i \omega_i^T$ with ω_i being the columns of Ω , and hence the rows of Y^{-1} by definition. \square

Lemma D.4. *Let $y_1, \dots, y_d \in \mathbb{R}^d$ be an orthonormal basis, and consider the linear map*

$$Z = \sum_{i=1}^n y_i y_i^T. \quad (46)$$

Then Z and its inverse Z^{-1} are both the identity matrix.

Proof. Since $Z y_i = \|y_i\|^2 y_i = y_i$ for all basis vectors, we see that Z is the identity matrix in this basis. But if a matrix is the identity in one basis, it's the identity in any basis. \square

D.3 Spherical random distribution

Now if the y_1, \dots, y_n are random vectors, we will provide conditions on the random distribution for the matrix Z to be invertible. We will see that it is the case for instance when the random distribution is spherical. Before we dive into this, let us recall some useful definitions and properties of the orthonormal transformations of a vector space \mathbb{R}^d .

First of all, recall that the orthonormal group is the set of matrices that preserve the euclidean distance, these matrices can be characterized by the property that they are invertible and that their inverse is equal to their transpose:

$$Q^T = Q^{-1}. \quad (47)$$

The orthogonal group encompasses the rotations of the space along with its reflections. Here is a technical lemma we will need related to the orthogonal transformations:

Lemma D.5. *If a matrix P is preserved by the group of orthogonal transformations, i.e., if*

$$P = Q^T P Q \quad (48)$$

for each orthogonal transformation Q , then the matrix is a multiple of the identity matrix, i.e., $P = cI$.

Proof. Let denote us by P_{ij} the entries of the matrix P . By using suitable orthonormal transformations as well as the relation $P = Q^T P Q$ we will first show that the off-diagonal elements of P_{ij} with $i \neq j$ must be zero. Then using a different orthonormal transformation, we will see that the diagonal elements need all to be one in order to satisfy $P = Q^T P Q$.

Let us start with the off-diagonal elements. Consider the orthonormal transformation Q that sends the basis vector e_i into the basis vector $-e_i$ and leaves all other basis vectors unchanged (reflection in the e_i direction). In coordinates, Q is the matrix with $Q_{il} = 1$ if $l \neq i$, $Q_{ii} = -1$ and all other entries set to zero. In this case, $P = Q^T P Q$ implies that

$$P_{ij} = \sum_{u,v} (Q^T)_{iu} P_{uv} Q_{vj}, \quad (49)$$

$$= \sum_{u,v} Q_{ui} P_{uv} Q_{vj}, \quad (50)$$

$$= Q_{ii} P_{ij} Q_{jj}, \quad (51)$$

$$= -P_{ij}, \quad (52)$$

$$(53)$$

and hence $P_{ij} = 0$ since zero is the only number which at the same time positive and negative. We can repeat this argument for any off-diagonal element.

Let us now take care of the diagonal elements knowing that the off-diagonal elements of P are zero. This means that $P = \text{diag}(c_1, \dots, c_d)$. Consider now the orthonormal operator Q that permutes the basis vector e_i with the basis vector e_j and leaves all other basis vectors unchanged (rotation in the ij -plane). In coordinates, Q is the matrix such that $Q_{ll} = 1$ if $l \neq i, j$, $Q_{ij} = Q_{ji} = 1$ and zero otherwise. Now with this transformation $P = Q^T P Q$ implies in coordinates that \square

$$P_{ii} = \sum_{u,v} (Q^T)_{iu} P_{uv} Q_{vi}, \quad (54)$$

$$= \sum_{u,v} Q_{ui} P_{uv} Q_{vi}, \quad (55)$$

$$= Q_{ji} P_{jj} Q_{ij}, \quad (56)$$

$$= P_{jj}, \quad (57)$$

$$(58)$$

and in other words that $c_i = c_j$. Since we can repeat this argument for any pair of basis vectors, we obtain that $P = cI$ where $c = c_1 = \dots = c_d$, which completes the proof.

Let us now define what we mean by a spherical random distribution of vectors.

Definition D.6. *We say that a random variable X has a spherical distributions when it is invariant under the orthogonal group; this means that X and its transformation by an element of the orthogonal group QX are identically distributed for any orthogonal transformation Q .*

We can infer a number of things just from the symmetrical aspect of a spherical distribution. For instance, it is easy to see that if a random variable is spherical, its mean is zero and its covariance matrix is a multiple of the identity. Namely, any other values would break the space symmetry.

The next lemma tells us that $Z = \sum_i y_i y_i^T$ is a multiple of the identity if the y_i 's come from a spherical random distribution, provided the number of samples is large enough.

Lemma D.7. *Consider the rank 1 operator $T_y = yy^T$, where y is a spherically distributed random variable on \mathbb{R}^d with covariance matrix $\sigma^2 I$. Then we have that the expectation of T_y is a multiple of the identity: i.e.,*

$$\mathbb{E}(T_y) = \sigma^2 I. \quad (59)$$

In particular, its empirical mean can approximate $\sigma^2 I$ arbitrarily close by increasing the number n of samples y_i of the random variable y :

$$\frac{1}{n} \sum_{i=1}^n y_i y_i^T \simeq \sigma^2 I. \quad (60)$$

Proof. Let Q be an orthogonal transformation. Since the distribution of the random variable y is spherical, it means that y and $z = Qy$ are identically distributed. Since both variables have the same distribution, then their associated rank 1 projectors $T_y = yy^T$ and $T_z = zz^T$ are also identically distributed. This implies in particular that they have identical means:

$$T := \mathbb{E}(T_y) = \mathbb{E}(T_z). \quad (61)$$

On the other hand, if we compute the expectation of T_z directly we obtain

$$\mathbb{E}(T_z) = \mathbb{E}(z^T z) \quad (62)$$

$$= \mathbb{E}(Q^T y^T y Q) \quad (63)$$

$$= Q^T \mathbb{E}(T_y) Q, \quad (64)$$

which implies that $T = Q^T T Q$ for all orthogonal matrix Q since $T = \mathbb{E}(T_y) = \mathbb{E}(T_z)$. Using now Lemma D.5, we conclude that $T = cI$ for a constant c . To determine the constant c above, we compute the trace of T_y using the cyclical property of the trace (i.e. $\text{trace}(AB) = \text{trace}(BA)$):

$$\text{trace}(T_y) = \text{trace}(y^T y) = \text{trace}(yy^T) = \text{trace}(\|y\|^2) = \|y\|^2. \quad (65)$$

Now taking the expectation on both sides of the equation $\text{trace}(T_y) = \|y\|^2$ and using that the expectation of the trace is the trace of the expectation, we obtain that

$$\mathbb{E}(\|y\|^2) = \text{trace}(Ic) \quad (66)$$

$$= c \text{trace}(I) \quad (67)$$

$$= cd. \quad (68)$$

Hence, we have that $c = \mathbb{E}(\|y\|^2)/d$ where d is the dimension of the space. Now, we can easily evaluate the expectation of $\|y\|^2$ using the expectation formula for a quadratic form: $\mathbb{E}(y^T A y) = E(y)^T A E(y) + \text{trace}(\Sigma A)$, where Σ is the covariance matrix for y . In our case, $E(y) = 0$ and $\Sigma = \sigma^2 I$ since the distribution is spherical. Therefore

$$\mathbb{E}(\|y\|^2) = \text{trace}(\sigma^2 I) = \sigma^2 d, \quad (69)$$

which gives us $c = \sigma^2$. □